JETIR.ORG ISSN: 2349-5162 | ESTD Year : 2014 | Monthly Issue
JOURNAL OF EMERGING TECHNOLOGIES AND INNOVATIVE RESEARCH (JETIR)
An International Scholarly Open Access, Peer-reviewed, Refereed Journal

Synthesis, Characterization, and Photocatalytic Application of Zn(II) Schiff Base Complex for Industrial Wastewater Treatment

[1]Mohammad Mudassir, [2]Ashish Kumar, [3]Mudit kumar gupta, [4]Shivalini Singh, [5]Himani Pachouri

[1]Research Scholar, [2]Professor, [2]Professor, [3]Research Scholar, [4]Research Scholar
Department of Chemistry, Agra College, Agra
Dr. Bhimrao Ambedkar University, Agra, India

***Abstract*:** This study reports the synthesis, characterization, and photocatalytic performance of a Zn(II) coordination complex for the treatment of industrial wastewater. The Schiff base ligand was synthesized by the condensation of 6-aminopenicillanic acid (6-APA) with salicylaldehyde and subsequently coordinated with Zn(II). The synthesized ligand and its metal complex were characterized using FTIR spectroscopy, ^{1}H NMR spectroscopy, UV-Visible and elemental analysis. The photocatalytic activity of the complex was evaluated using real car-wash industry's wastewater with initial total organic carbon (TOC) and UV_{254} values of 150 mg/L and 2.08 respectively. Under the reported experimental conditions, a catalyst dosage of 0.5 g/L resulted in TOC and UV_{254} removal efficiencies of 72.67 % and 59.1%, respectively, after 180 min of irradiation. These findings indicate the potential of the establish its practical applicability.

***Keyword*:** Schiff base, Photocatalytic degradation, wastewater treatment

1. INTRODUCTION

Air, water, and food are essential for human survival. Among these, water is indispensable for sustaining life and maintaining ecological balance. However, only about 2.5% of the Earth's total water is freshwater, and only a small fraction of this is readily available for human use **[1]**. Rapid industrialization has increased the discharge of pollutants into natural water bodies, contributing to water pollution. Dyes, pigments, and paints are widely used in industries such as textiles, leather processing, food production, paper manufacturing, and plastics. The wastewater generated by these industries may contain various pollutants that adversely affect aquatic ecosystems and environmental quality **[2, 3].**

Industrial wastewater containing organic pollutants requires effective treatment before its discharge into the environment. Therefore, developing efficient and economical methods to remove or degrade these contaminants is an important challenge in environmental remediation **[4].** Advanced oxidation processes (AOPs) have attracted considerable attention for wastewater treatment because they generate highly reactive species capable of oxidizing a wide range of organic pollutants **[5, 6].** Among these processes, Schiff base metal complexes, titanium dioxide (TiO_2)-based photocatalysis and photo-Fenton treatment are widely investigated approaches for the degradation of organic contaminants **[7, 8].** Schiff base ligands are commonly formed by condensation of a primary amine with a suitable carbonyl compound. Their donor atoms and molecular structures can be modified, making them useful in coordination chemistry **[9, 10].** Metal complexes containing Schiff base ligands have been studied in several catalytic and photochemical applications. However, the photocatalytic behaviour of an individual complex must be demonstrated experimentally and should not be inferred solely from the presence of a metal centre or UV–visible absorption bands.

Metal–organic complexes, including metal porphyrins and metal phthalocyanines, have been investigated as catalysts because of their ability to facilitate electron-transfer processes and, in suitable cases, absorb visible light. These properties can support the activation of molecular oxygen or hydrogen peroxide and promote oxidative reactions under appropriate conditions **[11].** Among various metal–organic compounds, Schiff base metal complexes have received considerable attention in catalysis because they can be prepared through relatively straightforward synthetic procedures and their coordination environments can be modified by changing the ligand

structure **[12].** Their electronic properties, coordination geometry, and catalytic behavior depend on factors such as the metal ion, donor atoms, ligand structure, and reaction conditions. Furthermore, modifications to the ligand framework can influence the stability, selectivity, and catalytic performance of these complexes **[13, 14]**. Schiff base complexes of transition metals, including copper, zinc and iron, have been investigated for the catalytic oxidation and photocatalytic degradation of organic compounds**.** Metal Schiff base complexes have also been explored in selective catalytic oxidation reactions under homogeneous conditions **[15]**. In comparison, heterogeneous catalytic systems offer the potential advantage of separating the catalyst from the treated wastewater, which may facilitate catalyst recovery and reuse. Certain catalyst structures may also help control aggregation and improve catalytic stability, although these properties depend on the specific material and experimental conditions **[16].**

Photocatalysis is a promising approach for wastewater treatment because light energy can initiate reactions that promote the degradation of organic contaminants. Solar irradiation is particularly attractive as a potentially sustainable energy source. Therefore, the development of efficient and reusable photocatalysts, including suitably designed Schiff base metal complexes, may provide a useful approach for the treatment of industrial wastewater.

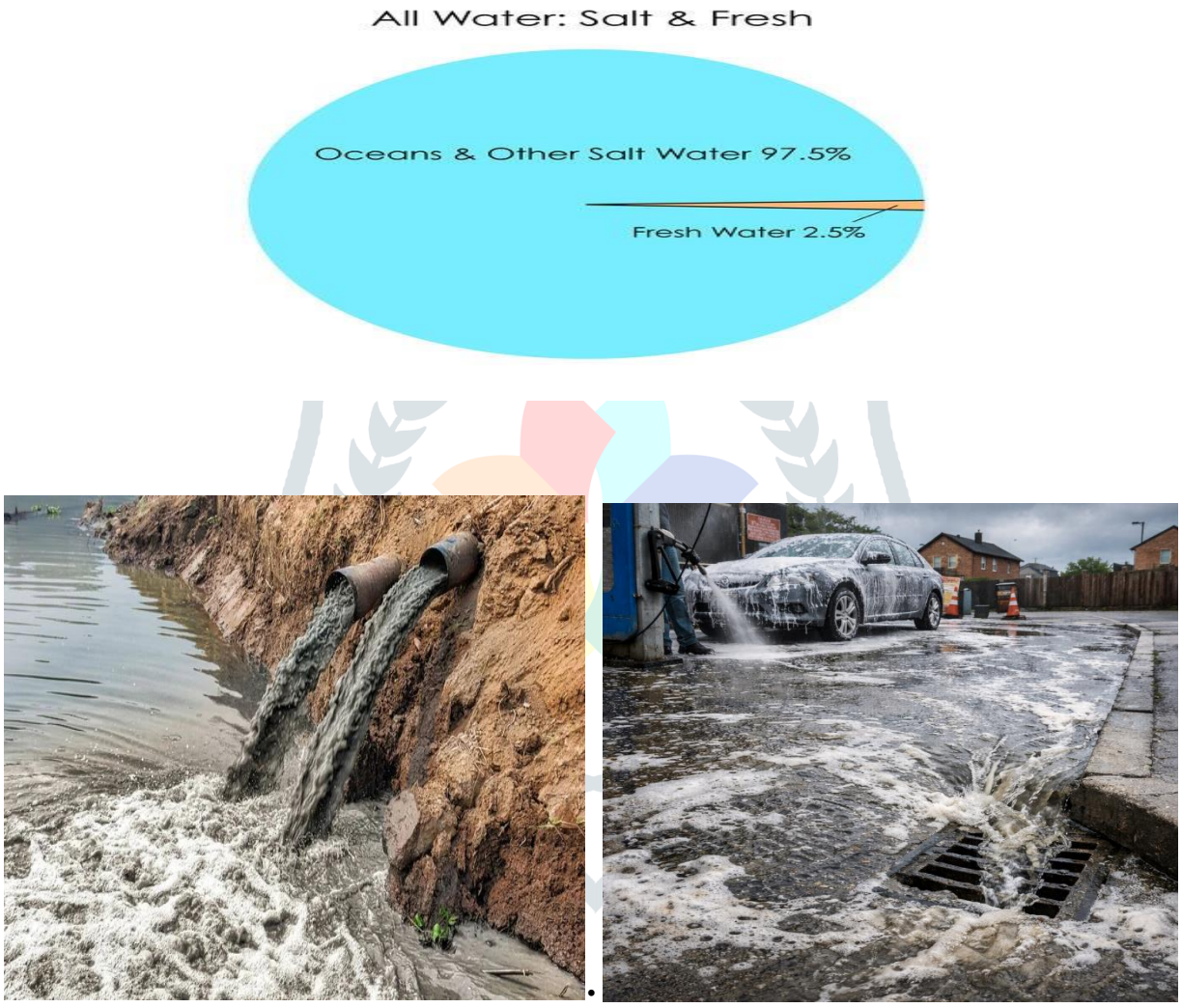

Fig.1. Pictures of water Pollution

2. Materials and method

2.1. Chemicals

Salicylaldehyde, 6-Aminopenicillanic Acid (6APA), methanol, ethanol, zinc acetate, Hydrochloric acid, sodium hydroxide. All reagents used were analytical grade, procured from CDH, Sigma Aldrich. All synthesis work was carried out in the Department of Chemistry, Agra College, Dr. Bhim Rao Ambedkar University, Agra.

2.2. Synthesis of Schiff base and metal complex

6-Aminopenicillanic acid (6-APA) (1 mmol, 0.216g) was suspended in 25ml of ethanol in a round bottom flask and salicylaldehyde (1 mmol, 0.122g) dissolved in 25ml of ethanol was added to individual suspension was added to the 6-APA suspension in 1:1 molar ratio. Reaction mixture stirred and refluxed at 60 °C for about 5-6 hours. After completion the reaction mixture was cooled to room temperature and the Schiff base ligand precipitated. The precipitate was filtered, washed several times with cold ethanol to remove the unreacted starting materials and dried under vacuum in a desiccator. The dried ligand was stored in sealed glass containers for subsequent characterization and complex synthesis. Initial purity and identity were confirmed by determining the melting point using a digital melting point apparatus.
IUPAC Name of ligand: (2S,5R)-6-(((E)-2-hydroxybenzylidene)amino)-3,3-dimethyl-7-oxo-4-thia-1-azabicyclo[3.2.0]heptane-2-carboxylic acid

2.3. Synthesis of and metal complex

6APA-Salicaldehyde (1 eq, 2mmol, 0.640g) was separately dissolved in 25 ml of ethanol. $Zn(CH_3COOH)_2$ (1eq, 1mmol, 0.183g) was dissolved in 25ml of ethanol and added to another flask containing 6APA-Salicylaldehyde. Reaction was occurred using metal salt and ligand ratio (1:2). The reactants were stirred at 60 °C for about 4-5 hours. After the reaction complication precipitated was cooled and filtered at room temperature. The resulting precipitated was stored in glass containers for further characterizations. Their melting points were identified by using a digital melting point apparatus for initial purity and primly characterization.

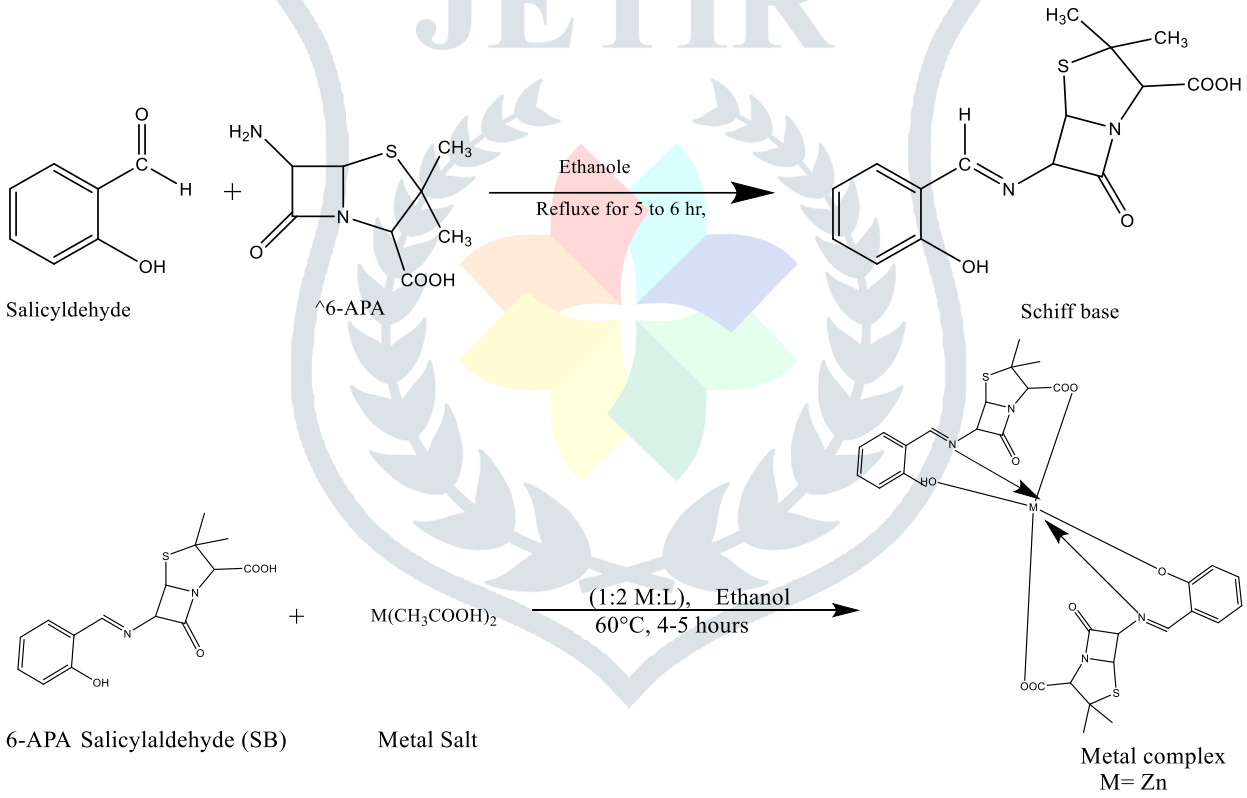

Fig.2. Synthesis Scheme of Schiff base ligand and complex

2.4. Characterization of ligand and complex

The reported characterization methods were FTIR, ^{1}H NMR, UV–visible spectroscopy, elemental analysis, TGA, and PXRD. The ligand ^{1}H NMR spectrums was recorded in DMSO.

2.5. Wastewater and photocatalytic experiment

Wastewater was collected from a car-washing facility. The reported initial values were pH 8.1, COD 650 mg/L, TOC 150 mg/L, UV254 absorbance 2.08 (au), TDS 1500 mg/L, and TSS 750 mg/L. The sampling date, collection protocol, storage conditions, analytical instruments, and standard methods were not specified fully in the source and should be added from laboratory records.

Experiments were conducted in a flat-bed, open-dish batch photoreactor inside a HEPA-filtered laminar-air-flow chamber. The reactor was irradiated using two 15 W UV-C lamps at a reported wavelength of 254 nm. Each run used 1 L of wastewater and Zn(II) complex loadings of 0.1, 0.3, or 0.5 g/L. The suspension was continuously stirred, and samples were collected after 60, 120, and 180 min. Experiments were reported in triplicate (n = 3). Lamp-to-sample distance, irradiance, temperature, sample-separation procedure, and analytical standard methods should be added if available.

2.6. Control and calculations

A catalyst-free UV-C control was performed under the same irradiation conditions without the Zn(II) complex. No dark-adsorption experiment was conducted; adsorption and light-driven contributions therefore cannot be quantified independently. Removal was calculated as:

$$\text{Removal } (\%) = [(C_0 - C_t) / C_0] \times 100$$

C_0 is the initial value and C_t is the value after irradiation time t. For UV254, the values refer to absorbance at 254 nm; for TOC, they refer to TOC concentration. Values are reported as mean ± standard deviation where supplied. The raw replicate data were not available in the manuscript file, so reported SDs should be checked against the original measurements. No ANOVA or p-value is claimed in this draft.

3. Result and Discussion

3.1. Elemental Analysis

Elemental analysis was performed to determine the percentage composition of carbon, hydrogen, nitrogen, sulphur, oxygen, and zinc in the synthesized Schiff base ligand and Zn(II) complex. The experimentally obtained values were compared with the theoretically calculated percentages based on their proposed molecular formulas

Table 1- Elemental analysis of Schiff base and metal complex

Ligands/Metal complex	Colour	M.P. (°C)	Yield	C Found (Calcd)	H Found (Calcd)	N Found (Calcd)	O Found (Calcd)	S Found (Calcd)	Zn Found (Calcd)	Mol. Wt. Found (Calcd)
6-APA Salicylaldehyde ($C_{15}H_{16}N_2O_4S$)	Lemon Yellow	107-109	81%	56.04 (56.24)	4.77 (5.03)	8.31 (8.74)	19.85 (19.98)	9.85 (10.01)	---	316.57 (320.36
$Zn(C_{15}H_{14}N_2O_4S)_2$ Brownish yellow solid	Brown yellow	151-153	58%	51.16 (51.18)	4.10 (4.29)	7.45 (7.96)	18.02 (18.18)	9.01 (9.11)	8.88 (9.29)	694.26 (702.07)

3.2. FTIR spectroscopy

3215 cm^{-1} (phenolic O–H stretching), **1755** cm^{-1} (β-lactam C=O stretching), **1645** cm^{-1} (azomethine C=N stretching),), **1290** cm^{-1} (C–N stretching), **1217** cm^{-1} (phenolic C–O stretching)

The azomethine (-C=N) stretching mode is responsible for the absorption band at 1645cm^{-1} in 2L ligand spectrum. This is a strong evidence of the production of imine linkages. Strong intramolecular hydrogen bonding in between (O–H) and (N=C} involving the phenolic hydroxyl group is responsible for the azomethine frequency shift to a lower wave number when compared to non-hydroxyl Schiff bases. The carbonyl (-C=O) stretching of the four-membered beta lactam ring is represented by a strong peak that appears at 1755 cm^{-1}, indicating that this did not undergo ring opening **[19]**. The presence of phenolic {OH} and {C–O} stretching modes is confirmed by the broad band around 3215 cm^{-1} and the strong band at 1217cm^{-1} respectively.

The FTIR spectra of Zn(6APA-Salicyldehyde)$_2$ complex was compared with that of the corresponding free ligand. The azomethine (C=N) stretching band shifts from 1645cm^{-1} to 1618 cm^{-1} upon complex formation, indicate possible coordination of the nitrogen donor atom with zinc **[18]**. Phenolic oxygen and carboxylic group oxygen band are also shift towards lower wavenumber, suggesting their possible involvement in coordination with the metal ion. The stretching band of phenolic oxygen and carboxylic oxygen shifts from 3215 cm^{-1} to 3173cm^{1}, and 1280cm^{-1} to 1275cm^{-1} respectively. The β-lactam C=O stretching vibration remains nearly unchanged after complexation that means C=O group does not participate in coordination. **[20]**. Evidence for metal–ligand bonding is provided by the emergence of new absorption bands in the spectra of the complexes which are assigned to M–N and M–O, modes. The ν(M–N) bands observed at 530 cm^{-1} and ν(M–O) bands observed 480 cm^{-1} **[21,22].**

Table 2- FTIR data (ν, cm^{-1}) of the ligand and zinc metal complex

Compounds name	ν C=N	ν C=O	ν C–O Stretch (-COOH / Carboxylate)	ν O–H Stretch (-COOH / Phenolic)	ν M-N	ν M-O
Ligand	1645	1755	1280	3215	-	-
Complex	1618	1755	1275	3173	530	480

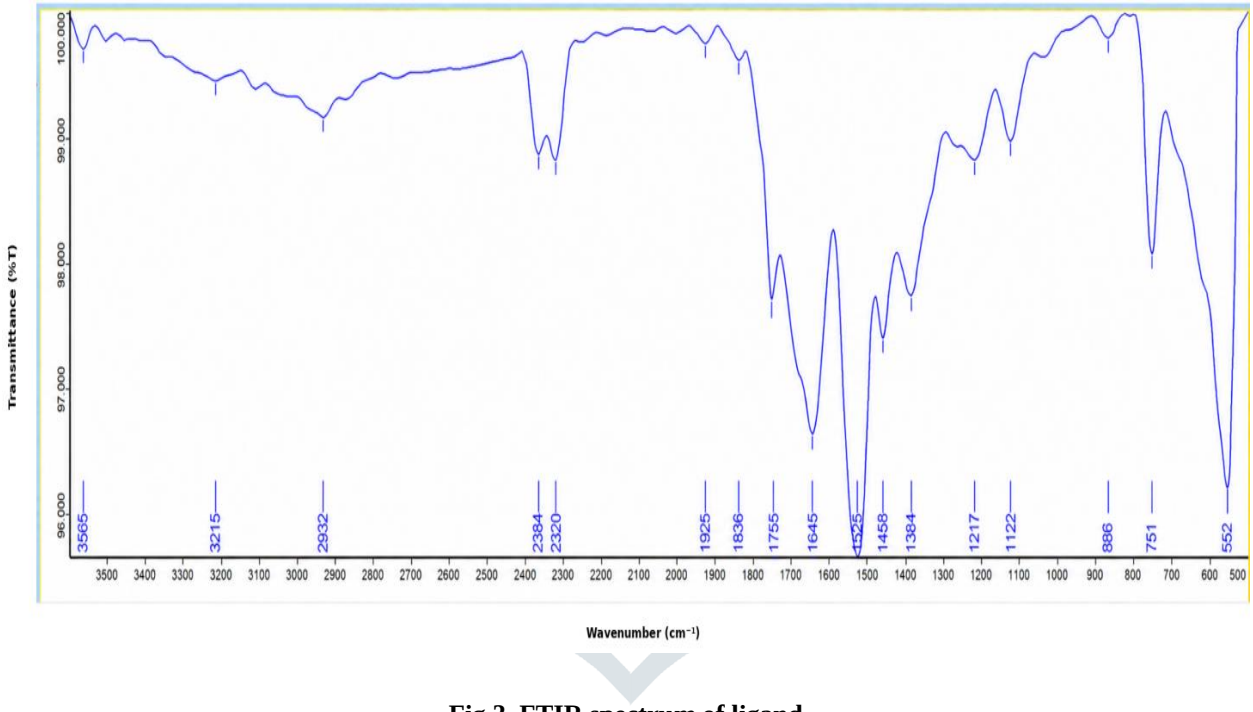

Fig 3. FTIR spectrum of ligand

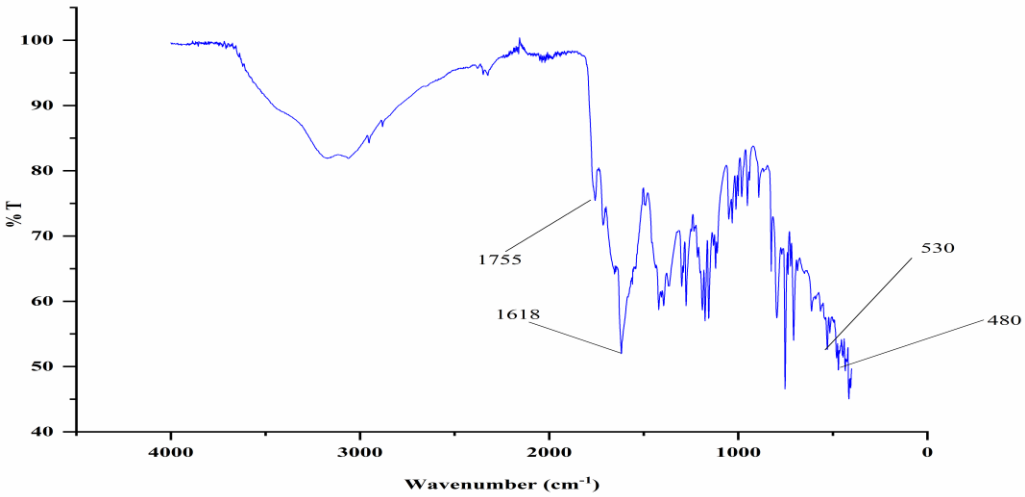

Fig 4. FTIR spectrum of complex

3.3. ^{1}H NMR spectroscopy

The ^{1}H NMR spectrum analysis of the ligand in DMSO showed a singlet peak at δ 8.73 ppm which was belongs to azomethine proton. Peaks for aromatic protons between δ 6.75 to 6.87 ppm, and for protons attached to the beta-lactam ring at δ 5.59 and δ 5.71 ppm. The appearance of these characteristic signals supports the synthesis of the Schiff base via the condensation reaction **[23].**

Table 3- NMR data of the ligand

LIGAND NAME	Azomethine -CH=N- (δ, ppm)	Aromatic Ar-H (δ, ppm)	β-Lactam Core Protons (δ, ppm)
(6-APA + Salicylaldehyde)	8.73 (s, 1H)	6.75–6.87 (m, 4H)	5.71 (d, 1H) 5.59 (d, 1H)

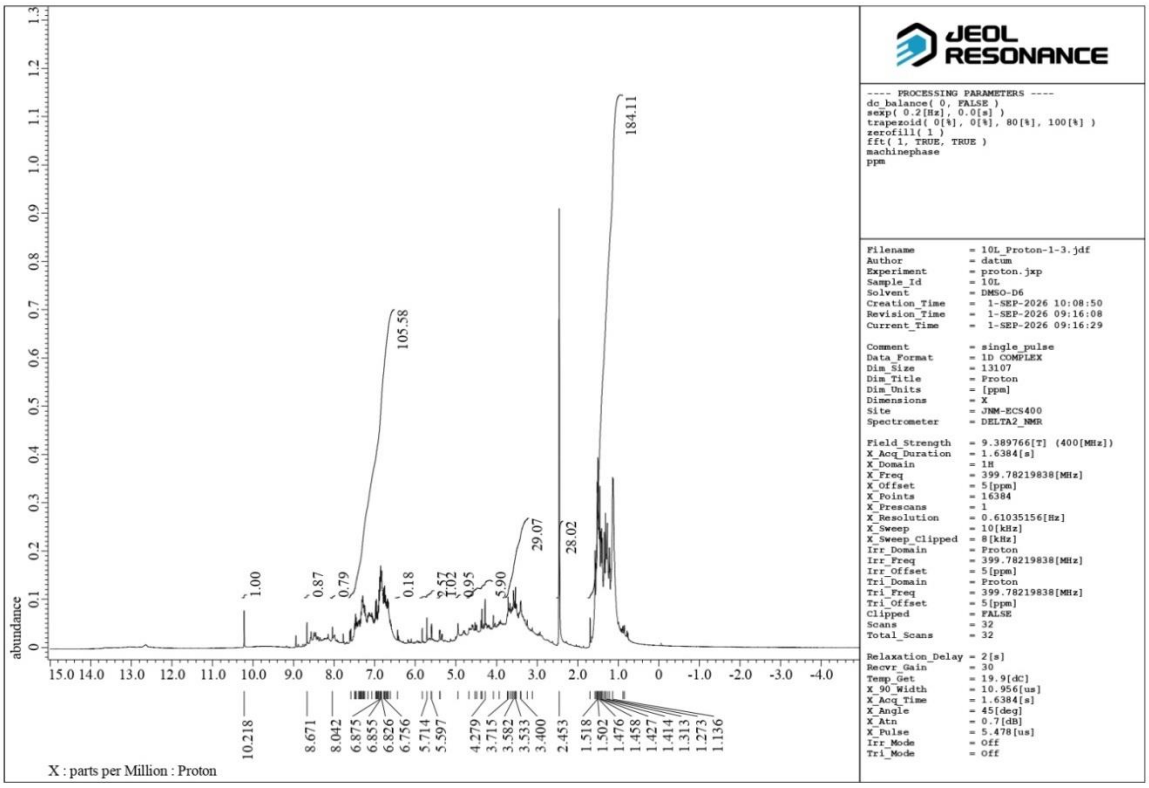

Fig 5. NMR Spectrum of ligand

3.4. UV-Visible spectroscopy

UV spectra of ligand exhibited three transitions at 226, 275 and 305 nm. The bands observed at 226 and 275nm are associated with π→π* transitions associated with aromatic system and conjugated azomethine group, respectively. Transition Band at 305 may be associated with n→π* transition ascribed to azomethine nitrogen's lone pair.These spectral features are consistent with an octahedral coordination geometry around the Zn(II) center **[24].** Complex exhibited absorption peaks at λ_{max} 273 nm, and 322 nm, are assigned to LMCT. These observations suggest an octahedral geometry around the Zn ion.

Table 4- UV data of the ligand and complex

Ligand	226, 275, 305	π-π* and n-π*	Aromatic ring core, Azomethine linkage
Complex	273, 322	LMCT	Octahedral

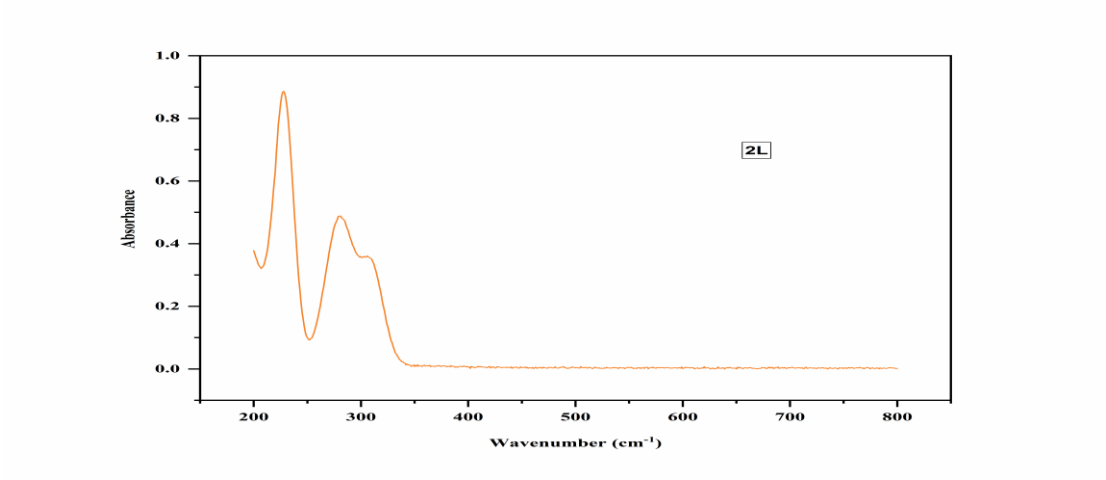

Fig 6. UV Spectrum of ligand

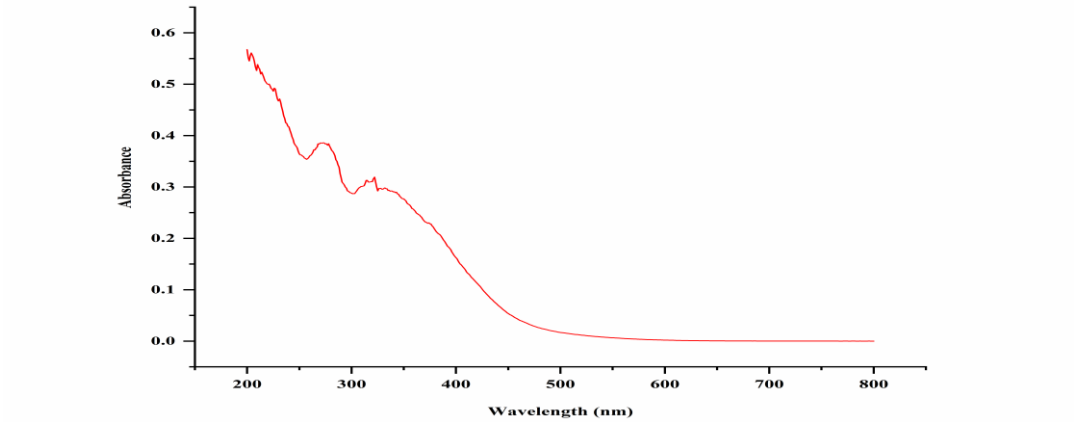

Fig 7. UV Spectrum of complex

3.5. Thermogravimative analysis

Complex, $Zn(C_{15}H_{14}N_2O_4S)_2$ (molecular weight 702.07) has been subjected to thermogravimetric analysis (TGA) in the temperature range 30-900 ºC. The study indicated many episodes of mass loss **[25].** The mass was reduced from 100% to about 95.0% between 30 and 150 °C, which demonstrated the weight loss of roughly 5.0% that can be attributed to the loss of adsorbed moisture. The second stage (150–220 °C) resulted in the loss of around 83.9% of the weight, which corresponds to 11.1% loss of mass, which is attributed to the heat degradation of initial thermal decomposition of complex. The disintegration stage was considerable in the range of 220-400 °C with a weight loss about 48% which corresponds to major loss of Schiff base organic framework **[26].** The large drop shows severe degradation of the ligand, notably the azomethine portion. The compound was decomposed slowly from 400 °C and weight loss continued 23.9% at 900 °C. The mass loss is ascribed to ongoing breakdown and carbonization of the organic material, leading to thermally stable zinc containing inorganic residue. Finally, 12.00% of the original mass remained as residue, very near to the theoretical residue for ZnO (11.56%) calculated from the molecular formula, verifying the formulation of complex and the presence of a zinc oxide-containing residue.

. **Table 5- TGA data of complex**

Phase	Temperature Range (°C)	Mass Loss (%)	Thermal Decomposition / Assignment
I	30-150	5.0	Loss of moisture/volatile impurities
II	150-350	11.1	Initial decomposition of complexe
III	350-800	48	Decomposition of Schiff base organic frame work
IV	800-900	23.9	Slow decomposition of remaining organic material
Final residue		**12.00**	**Stable metal oxide residue**

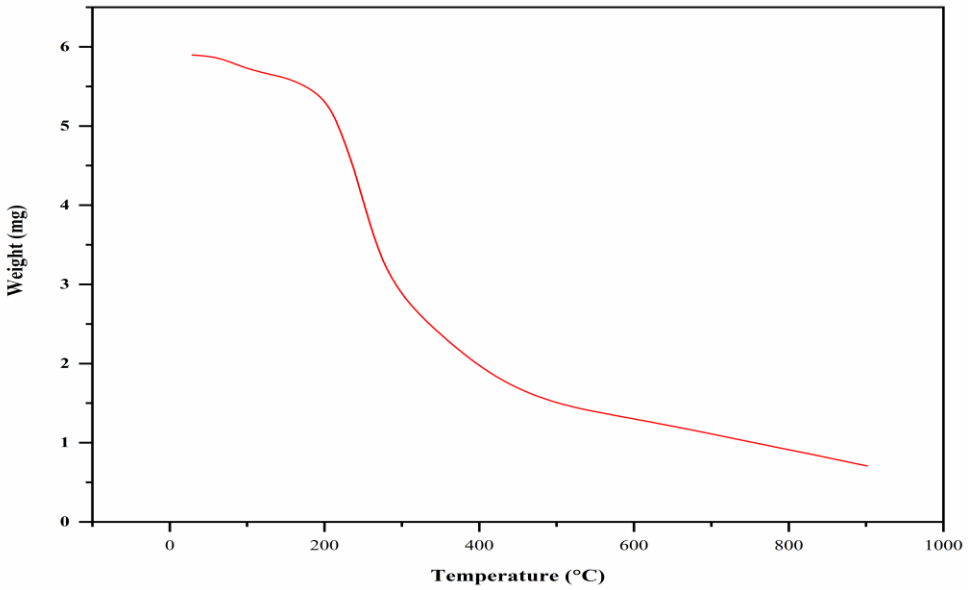

Fif 8. TGA spectrum of complex

3.6. PXRD and Crystal Size

The XRD pattern of complex displayed several strong diffraction peaks, which are the characteristics of the crystalline nature of complex. The maximum diffraction peak was obtained at 2θ = 17.9559° with relative intensity of 100 %. The FWHM of this peak was found to be 0.176896 degree which is equal to a beta value of 0.003087 rad. The size of the crystallite was determined by utilizing Scherrer equation **[27].** The form factor (K) employed was 0.9 and Cu-Kα radiation (λ = 0.15406 nm) was used. The average crystallite size of is calculated to be about 45.43 nm.

Table 6 - PXRD data of complex

Complex	2θ	Crystallite size
Zn(6-APA Salicylaldehyde)	17.95 degree	45.43nm

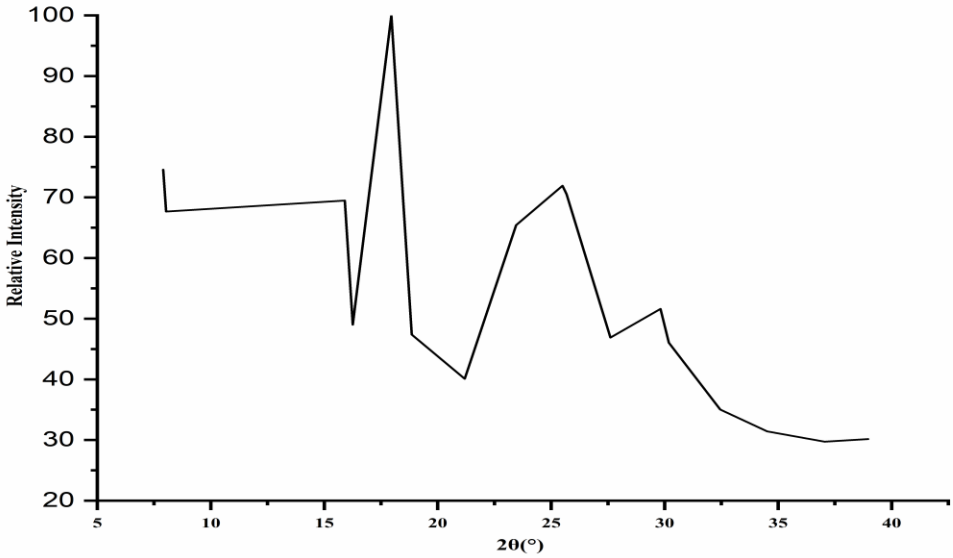

Fig 9. PXRD Spectrum of complex

3.7. Industrial Waste water Matrix for car wash factory

The high concentration of total suspended solids suggests the presence of a large amount of particulate matter, which is typical of car wash wastewater.

Table 7- physic-chemical parameters of untreated waste water

Parameter	Value	Indication
pH	8.1	The wastewater was slightly alkaline in nature.
COD	650 mg/L	The high COD value indicates a significant organic load due to the presence of detergents, oil and grease, and hydrocarbons.
TOC	150 mg/L	The wastewater contained a considerable amount of organic carbon.
UV_{254}	2.08	Presence of UV-absorbing constituents, including potentially some organic

Parameter	Value	Indication
		compound
TDS	1500 mg/L	The elevated total dissolved solids indicate a high concentration of dissolved salts, detergents, and other soluble contaminants.
TSS	750 mg/L	Indicates a substantial amount of suspended particulate matter, including soil, sand, and vehicle-derived residues.

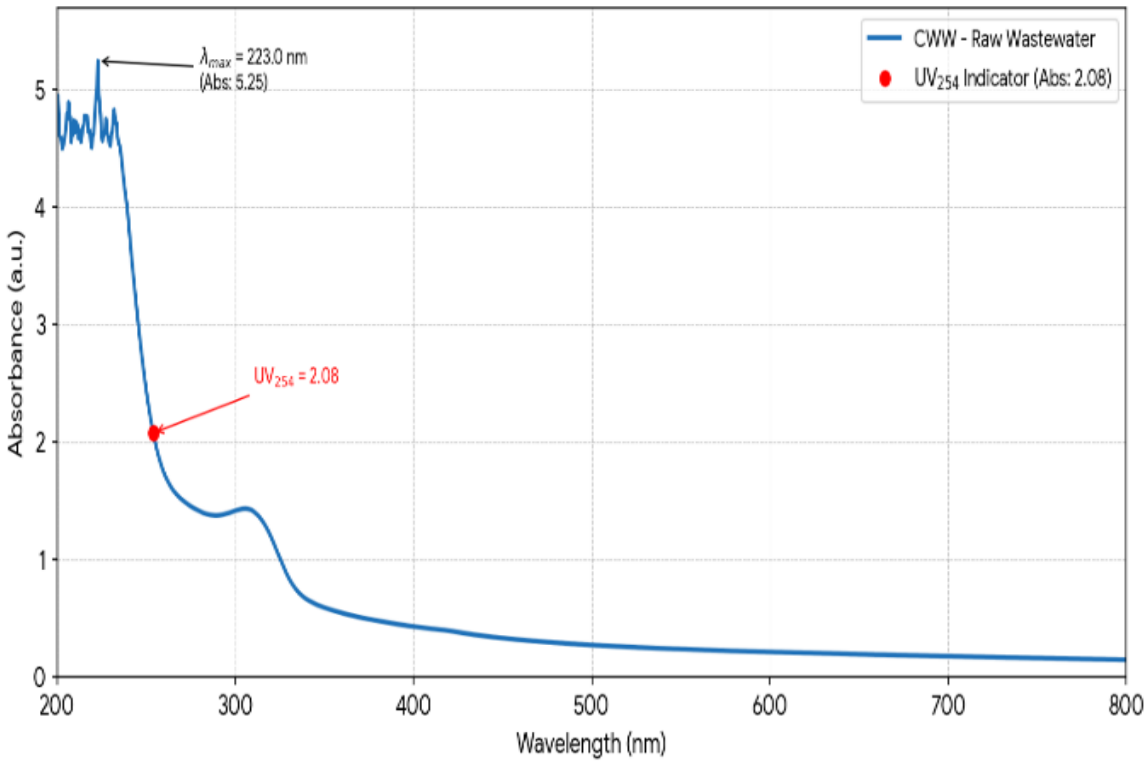

Fig 10. UV- visible absorption spectrum of raw water

The wastewater showed a high COD (650 mg/L) and TOC (150 mg/L). The COD/TOC ratio (~4.3) indicates the presence of large amounts of chemically oxidizable pollutants such as detergents, surfactants, oils, and petroleum hydrocarbons, requiring advanced treatment. The UV–Vis absorption spectrum showed strong absorption in the ultraviolet region, particularly between 200 and 230 nm, followed by a marked decrease in absorbance at higher wavelengths. These findings indicate the presence of organic carbon and UV-absorbing constituents in the wastewater. High TSS and TDS: The TSS (750 mg/L) reflects the presence of suspended particles like soil, sand, and vehicle debris, while TDS (1500 mg/L) confirms high concentrations of dissolved salts and cleaning chemicals. The wastewater had a pH of 8.1**,** due to the use of alkaline detergents and commercial cleaning agents during vehicle washing. The high organic load, elevated solids, and alkaline pH indicate that car wash wastewater requires efficient treatment. These characteristics support the application of Schiff base metal complex-based photocatalytic oxidation for effective pollutant degradation.

Photo catalytic Activity of Zn(6APA-Salicylaldehyde) complexes generally exhibit photocatalytic activity. The phenolic –OH group provides an additional coordination site to the metal ion. Ligand-to-metal charge transfer (LMCT) is enhanced, facilitating efficient electron transfer. The generation of hydroxyl radicals (•OH) is increased, resulting in more effective oxidation of organic pollutants. Electron-hole recombination is suppressed, thereby improving the overall photocatalytic efficiency.

$[Zn^{II}(L)] + hv \rightarrow [Zn^{II}(L)]^{*} + e^{-}$ ……..(1)
$O_2 + e^{-} \rightarrow O_2\bullet^{-}$ …… (2)
$O_2\bullet^{-} + H^{+} \rightarrow HO_2^{\bullet}$ …….. (3)
$2HO_2\bullet \rightarrow H_2O_2 + O_2$ ……. (4)
$H_2O_2 + e^{-} \rightarrow {}^{\bullet}OH + OH^{-}$ …… (5)

•OH + Organic pollutants → Intermediate products (6)

Intermediate products (Further oxidation) → $CO_2 + H_2O$ + Inorganic ions ……. (7)

3.8. Direct UV-C photolysis (Catalyst free)

To quantify the contribution of direct photolysis, i.e., pollutant breakdown by UV-C photons alone, without any catalyst, a control experiment was run under identical irradiation conditions (15 W UV-C, laminar air flow) but with no Schiff base metal complex present. Direct UV-C photolysis showed a gradual increase in both TOC and UV_{254} removal with irradiation time. After 180 min, TOC removal reached 8.2%, whereas UV_{254} removal reached 18.7%. The higher reduction in UV_{254} absorbance than in TOC suggests that UV-C irradiation affected UV-absorbing organic compounds more strongly than it mineralized the total organic carbon.

Table 8- TOC and UV_{254} Removal ± SD

Time	60min	120min	180min
TOC± SD	143.70 ± 3.30	140.55 ± 3.30	137.70 ± 3.30
U_{V254}± SD	1.916 ± 0.040	1.783 ± 0.040	1.691 ± 0.040

Table 9 - Removal of TOC and UV254 UV-C photolysis (no catalyst) (%)

Time (min)	TOC Removal	UV254 Removal
60	4.20%	7.9%
120	6.3%	14.3%
180	8.2%	18.7%

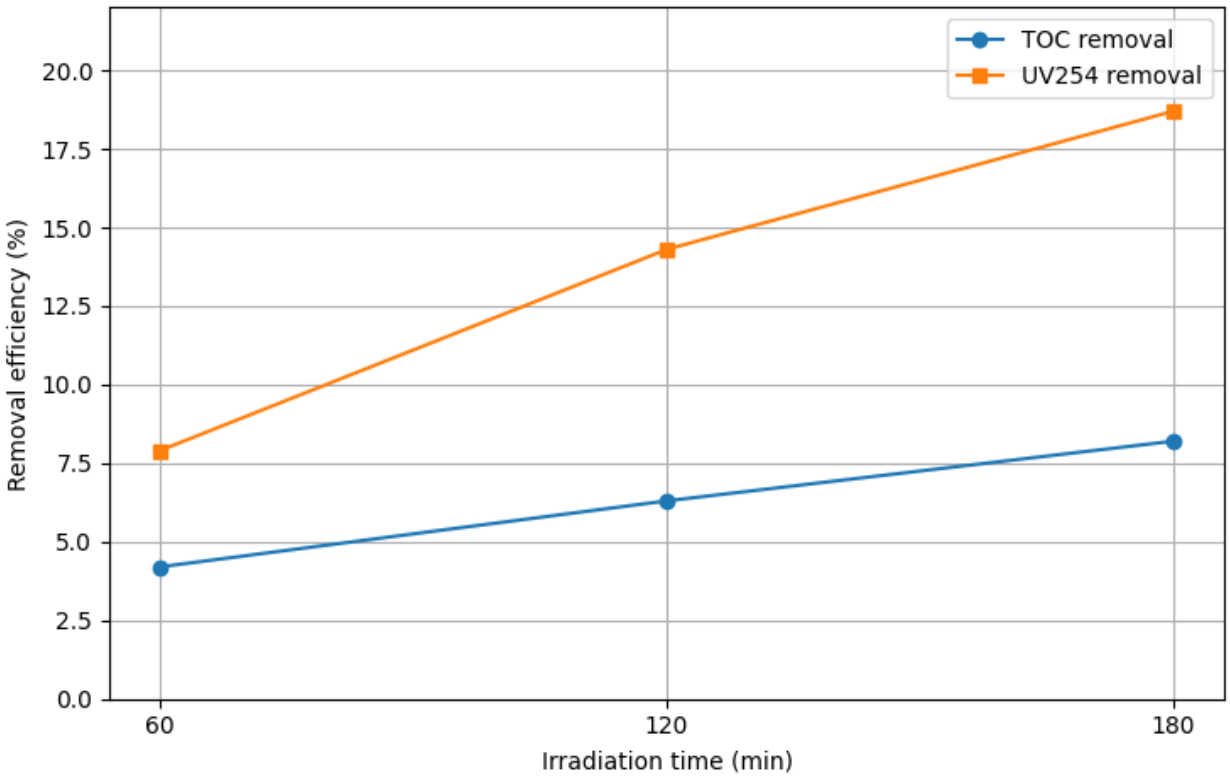

Fig 10. Direct UV-C photolysis (catalyst free)

3.9. Photo Catalytic Degradation

With both the catalyst and the UV-C source active, degradation of TOC and UV_{254} was markedly faster and more extensive than photolysis alone, confirming a strong synergy between the Schiff base metal catalyst and UV-C irradiation. The sub-sections below discuss the principal trends with respect to irradiation time, catalyst dose and dopant type, focusing on the optimum catalyst dose of 0.5g/L.

The UV254 removal efficiency was calculated from the decrease in absorbance at 254 nm relative to the initial absorbance of the wastewater. The results are expressed as mean ± standard deviation (SD) of triplicate measurements (n = 3). An increase in UV254 removal with irradiation time indicates a reduction in UV-absorbing organic compounds, including aromatic and conjugated substances. The extent of UV254 removal varied with catalyst dosage, suggesting that the amount of catalyst influenced the treatment efficiency under the investigated conditions. However, a decrease in UV254 absorbance does not necessarily indicate complete mineralization of organic pollutants; therefore, the results should be interpreted alongside TOC removal data.

3.9. UV254 response to catalyst loading and irradiation time

With the complex and UV-C irradiation, UV254 absorbance decreased with time. At each sampling time, the lowest residual absorbance was reported at 0.5 g /L. After 180 min, absorbance values were 1.230, 1.020, and 0.850 at 0.1, 0.3, and 0.5 g/ L, respectively, corresponding to reductions of 40.9%, 51.0%, and 59.1% from the initial value of 2.08. The trend indicates improved UV254 reduction as the catalyst loading increased within the tested range **[28]**.

Table 10- UV_{254} Removal ± SD

Complex	Dose (g/L)	60 min	120 min	180 min
Zn(6APA–Salicylaldehyde)	0.1	1.750 ± 0.006	1.480 ± 0.007	1.230 ± 0.005
Zn(6APA–Salicylaldehyde)	0.3	1.600 ± 0.004	1.310 ± 0.007	1.020 ± 0.004
Zn(6APA–Salicylaldehyde)	0.5	1.480 ± 0.006	1.170 ± 0.006	0.850 ± 0.005

Table 11- UV_{254} Removal Percentage (%)

Complex	Dose (g/L)	60 min	120 min	180 min
Zn(6APA–Salicylaldehyde)	0.1	15.9	28.8	40.9
Zn(6APA–Salicylaldehyde)	0.3	23.1	37.0	51.0
Zn(6APA–Salicylaldehyde)	0.5	28.8	43.8	59.1

3.10. TOC response to catalyst loading and irradiation time

The TOC value decreased as the irradiation time and catalyst loading increased. After 180 minutes, TOC decreased from 150 mg/L to 79 mg/L at 0.1 g/L catalyst loading, showing 47.33% removal. At 0.3 g/L, TOC decreased to 56 mg/L (62.67% removal). The best result was obtained at 0.5 g/L, where TOC decreased to 41 mg/L, giving 72.67% removal. The catalyst-containing tests showed larger TOC and UV254 reductions than the catalyst-free UV-C control. This supports improved treatment performance in the presence of the complex under the tested conditions **[29].**

Table 12- TOC Removal ± SD

Catalyst Complex	Dose (g/L)	60 min	120 min	180 min
Zn(6APA–Salicylaldehyde)	0.1	128.0 ± 1.9	100.0 ± 1.7	79.0 ± 1.6
Zn(6APA–Salicylaldehyde)	0.3	111.0 ± 1.8	78.0 ± 1.6	56.0 ± 1.5
Zn(6APA–Salicylaldehyde)	0.5	96.0 ± 1.7	61.0 ± 1.5	41.0 ± 1.4

Table 13- TOC Removal Percentage (%)

Catalyst Complex	Dose (g/L)	60 min	120 min	180 min
Zn(6APA–Salicylaldehyde)	0.1	14.67	33.33	47.33
Zn(6APA–Salicylaldehyde)	0.3	26.00	48.00	62.67
Zn(6APA–Salicylaldehyde)	0.5	36.00	59.33	72.67

3.11. Photocatalytic Reactor and Experimental Design

Photocatalytic degradation experiments were carried out in a flat-bed, open-dish batch photo reactor housed inside a HEPA-filtered laminar air-flow (LAF) chamber to minimize external contamination. The reactor was irradiated using two 15 W UV-C lamps (λ = 254 nm). For each experiment, 1 L of car washing factory wastewater was treated with the synthesized Zn(6APA–salicylaldehyde) Schiff base complex at catalyst dosages of 0.1, 0.3, and 0.5 g per 1 lit. The reaction mixture was continuously stirred, and aliquots were collected at 60, 120, and 180 min for physicochemical analysis. All experiments were conducted in triplicate (n = 3)

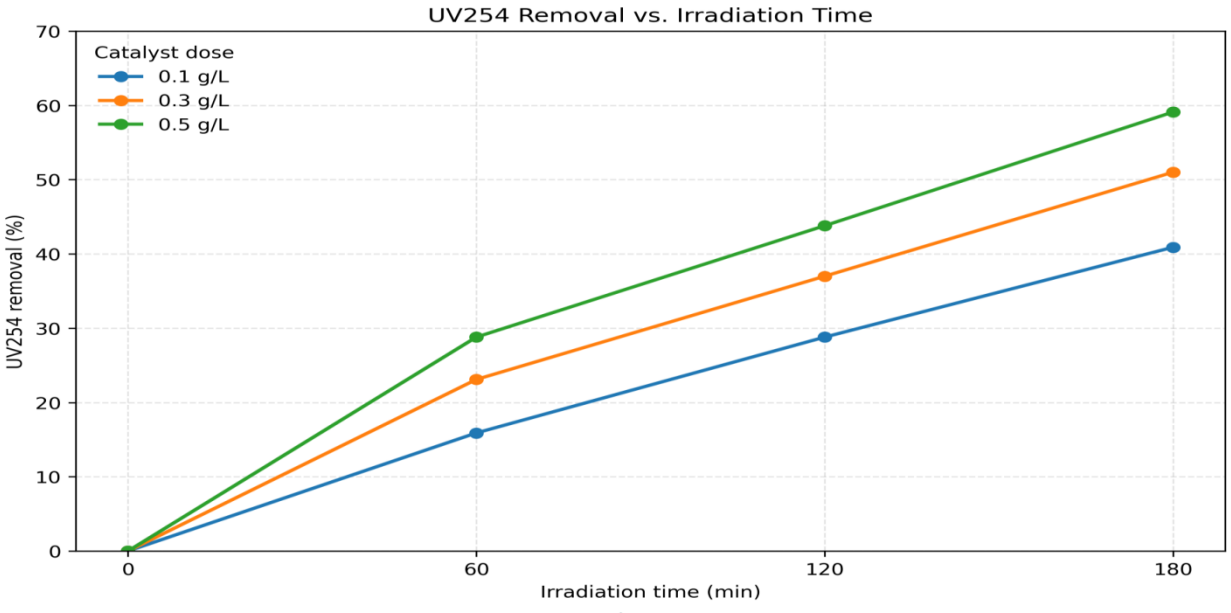

Fig 11. Removal of UV_{254} v/s irradiation time (min)

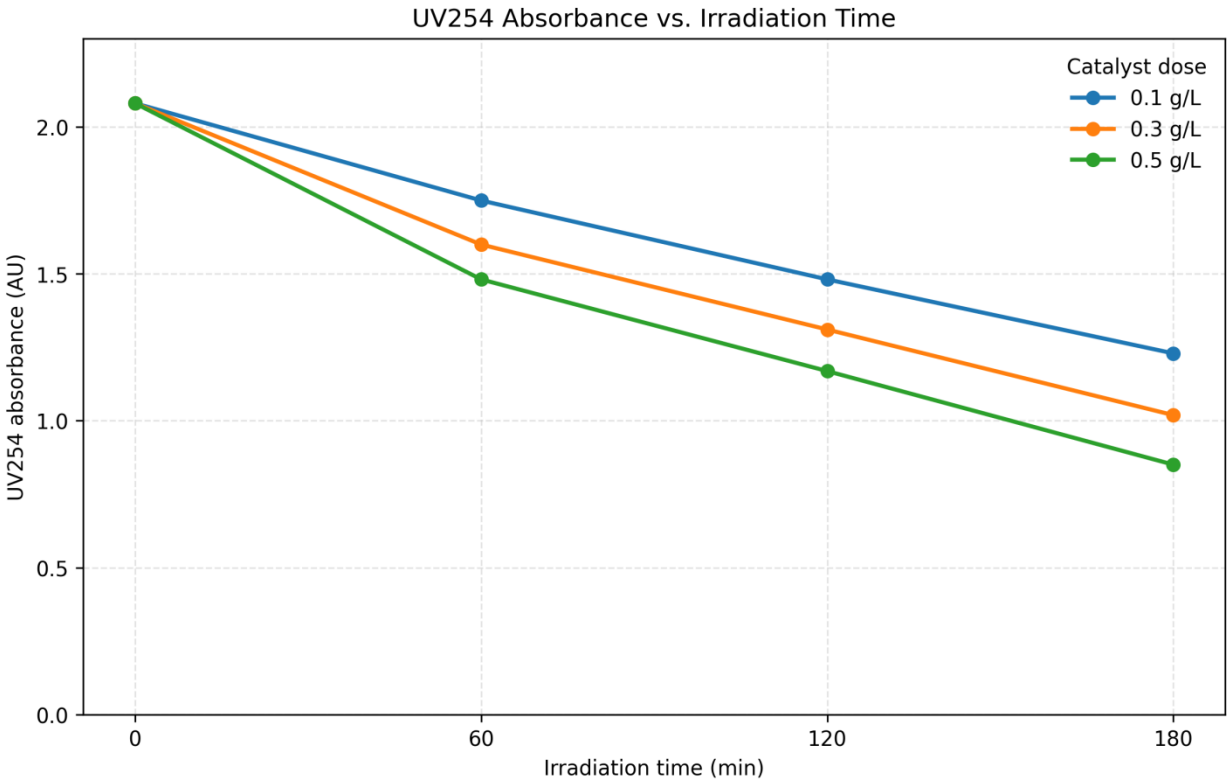

Fig 12. Absorbance of UV_{254} v/s irradiation time(min)

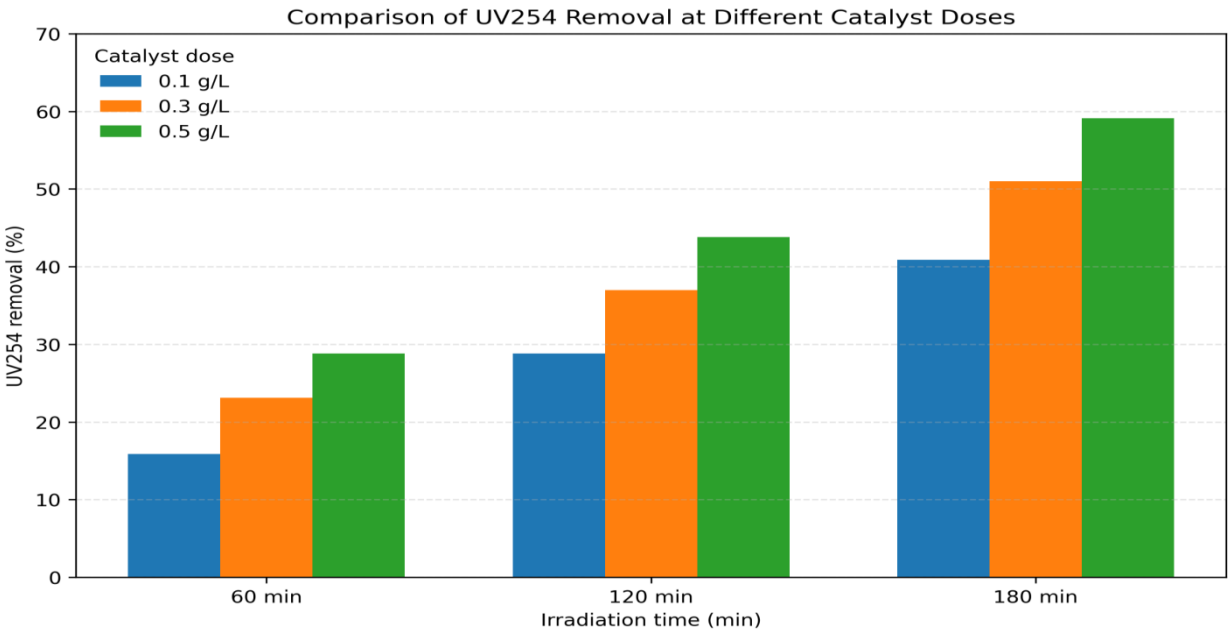

Fig 13. Comparison of UV_{254} removal at different doses

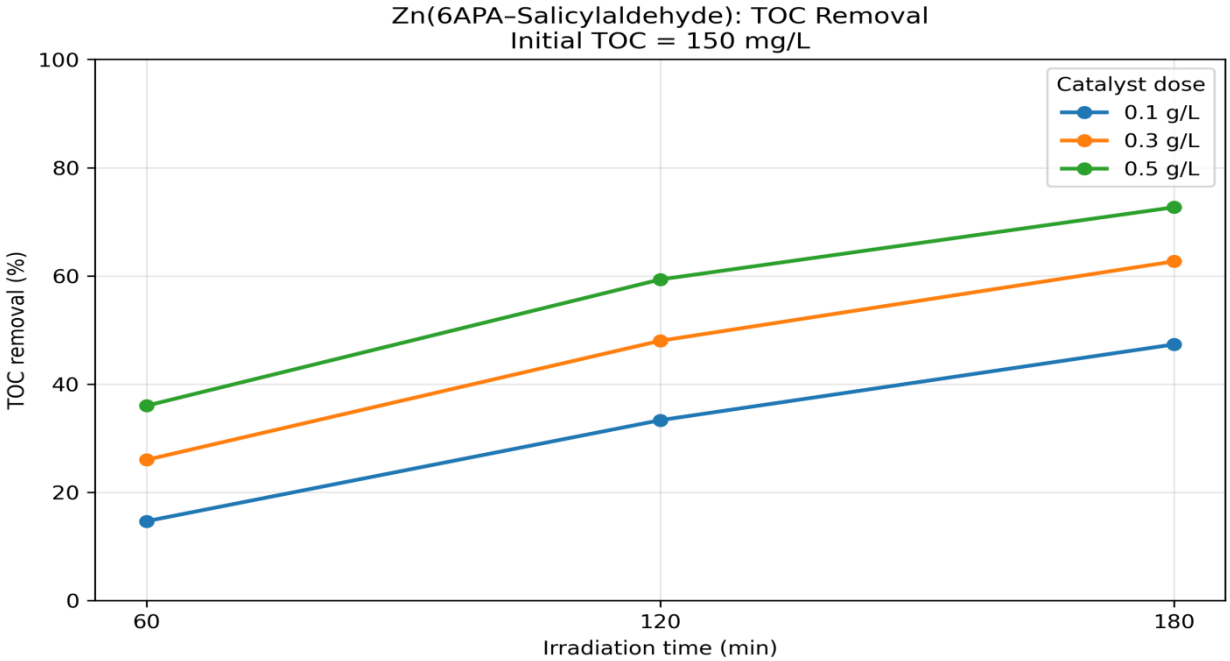

Fig 14. Removal of TOC v/s irradiation time (min)

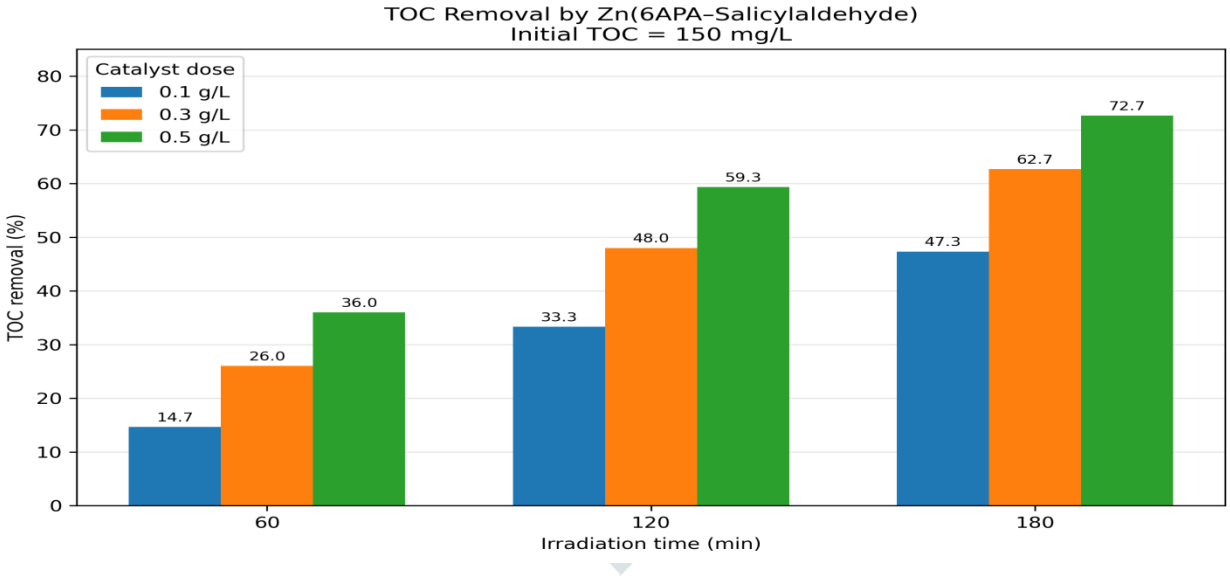

Fig 15. Comparison of TOC removal at different doses

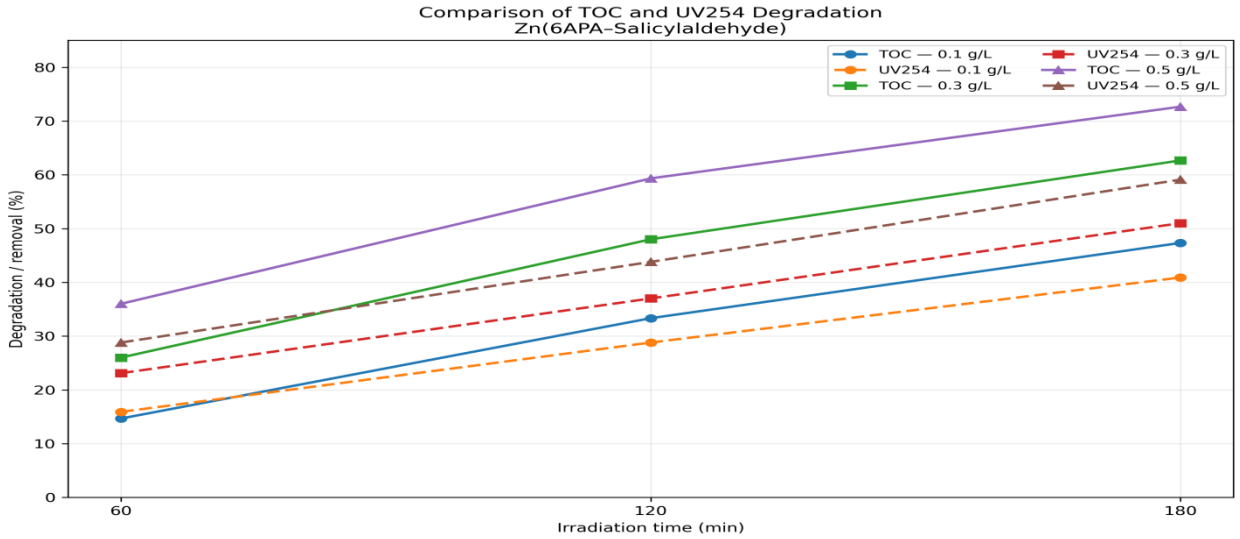

Fig 16. Comparison of TOC and UV_{254} degradation

4. CONCLUSION

6-APA-salicylaldehyde Schiff base ligand-coordinated Zn(II) complexes, synthesized via a controlled condensation and reflux route, were systematically evaluated as heterogeneous photocatalysts for the remediation of real-time industrial car wash wastewater. Coordination of the Zn(II) metal core with the rigid ONO-donor Schiff base scaffold significantly enhanced the structural and electronic characteristics, facilitating efficient ligand-to-metal charge transfer (LMCT) and suppressing photogenerated electron-hole recombination. Under optimized operational parameters at a catalyst loading of 0.5g/L and 180 min of light exposure, Total Organic Carbon (TOC) mineralization efficiency of 72.67 % reducing residual organic carbon from an initial 150 mg/L down to 41 mg/L and UV254 reduced to 59.1 % . A catalyst-free UV-C photolysis experiment was carried out under the same irradiation conditions to determine how much pollutant removal occurred due to UV light alone. The results were then compared with those obtained using the Zn(II) complex under UV-C irradiation. This comparison helped show the improvement in pollutant removal in the presence of the catalyst. However, since a dark-adsorption experiment was not performed, the contribution of pollutant adsorption onto the catalyst surface could not be determined separately.

5. ACKNOWLEDGMENT

The authors thank the Department of Chemistry, Agra College, Dr. Bhimrao Ambedkar University, Agra, LBS college, Jaipur, and MNIT, Jaipur for synthesis facilities and support.

REFERENCES

1. Tindall, J. A., Campbell, A. A., & Moran, E. H. (2010, December). Water security-national and global issues. In *AGU Fall Meeting Abstracts* (Vol. 2010, pp. H14F-01).

2. Lin, J., Ye, W., Xie, M., Seo, D. H., Luo, J., Wan, Y., & Van der Bruggen, B. (2023). Environmental impacts and remediation of dye-containing wastewater. *Nature Reviews Earth & Environment*, *4*(11), 785-803.

3. Wang, X., Jiang, J., & Gao, W. (2022). Reviewing textile wastewater produced by industries: characteristics, environmental impacts, and treatment strategies. *Water Science and Technology*, *85*(7), 2076-2096.

4. Mukherjee, J., Lodh, B. K., Sharma, R., Mahata, N., Shah, M. P., Mandal, S., ... & Bhunia, B. (2023). Advanced oxidation process for the treatment of industrial wastewater: A review on strategies, mechanisms, bottlenecks and prospects. *Chemosphere*, *345*, 140473.

5. Miklos, D. B., Remy, C., Jekel, M., Linden, K. G., Drewes, J. E., & Hübner, U. (2018). Evaluation of advanced oxidation processes for water and wastewater treatment–A critical review. *Water research*, *139*, 118-131.

6. Ma, D., Yi, H., Lai, C., Liu, X., Huo, X., An, Z., ... & Yang, L. (2021). Critical review of advanced oxidation processes in organic wastewater treatment. *Chemosphere*, *275*, 130104.

7. Das, A., Adak, M. K., Mahata, N., & Biswas, B. (2021). Wastewater treatment with the advent of TiO2 endowed photocatalysts and their reaction kinetics with scavenger effect. *Journal of Molecular Liquids*, *338*, 116479.

8. Goswami, N., & Barman, P. (2025). Schiff base metal complexes as alternative heterocatalysts in water remediation: Photocatalytic degradation of toxic organic pollutants. *Journal of Molecular Structure*, 143925.

9. Cozzi, P. G. (2004). Metal–Salen Schiff base complexes in catalysis: practical aspects. *Chemical Society Reviews*, *33*(7), 410-421.

10. Kanwal, A., Parveen, B., Ashraf, R., Haider, N., & Ali, K. G. (2022). A review on synthesis and applications of some selected Schiff bases with their transition metal complexes. *Journal of coordination chemistry*, *75*(19-24), 2533-2556.

11. Zhang, R., & Warren, J. J. (2021). Recent developments in metalloporphyrin electrocatalysts for reduction of small molecules: strategies for managing electron and proton transfer reactions. *ChemSusChem*, *14*(1), 293-302.

12. Juyal, V. K., Pathak, A., Panwar, M., Thakuri, S. C., Prakash, O., Agrwal, A., & Nand, V. (2023). Schiff base metal complexes as a versatile catalyst: A review. *Journal of organometallic chemistry*, *999*, 122825.

13. Malav, R., & Ray, S. (2025). Recent advances in the synthesis and versatile applications of transition metal complexes featuring Schiff base ligands. *RSC advances*, *15*(28), 22889-22914.

14. Liu, X., Manzur, C., Novoa, N., Celedón, S., Carrillo, D., & Hamon, J. R. (2018). Multidentate unsymmetrically-substituted Schiff bases and their metal complexes: Synthesis, functional materials properties, and applications to catalysis. *Coordination Chemistry Reviews*, *357*, 144-172.

15. Ramnauth, R., Al-Juaid, S., Motevalli, M., Parkin, B. C., & Sullivan, A. C. (2004). Synthesis, structure, and catalytic oxidation chemistry from the first oxo− imido schiff base metal complexes. *Inorganic chemistry*, *43*(13), 4072-4079.

16. Ahmed, S. N., & Haider, W. (2018). Heterogeneous photocatalysis and its potential applications in water and wastewater treatment: a review. *Nanotechnology*, *29*(34), 342001.

17. Iqbal, M. A., Akram, S., Lal, B., Hassan, S. U., Ashraf, R., Kezembayeva, G., ... & Hosseini-Bandegharaei, A. (2024). Advanced photocatalysis as a viable and sustainable wastewater treatment process: A comprehensive review. *Environmental Research*, *253*, 118947.

18. Pavia, D. L., Lampman, G. M., Kriz, G. S., & Vyvyan, J. R. (2001). Introduction to spectroscopy. *Belmont, USA*, *13*-60.

19. Nawar, N., & Hosny, N. M. (2000). Synthesis, spectral and antimicrobial activity studies of o-aminoacetophenone o-hydroxybenzoylhydrazone complexes. *Transition Metal Chemistry*, *25*(1), 1-8.

20. Geary, W. J. (1971). The use of conductivity measurements in organic solvents for the characterisation of coordination compounds. *Coordination Chemistry Reviews*, *7*(1), 81-122.

21. Bellamy, L. J. F. C. (2013). The infra-red spectra of complex molecules. *Springer Science & Business Media*.

22. Nakamoto, K. (2009). Infrared and Raman spectra of inorganic and coordination compounds, part B: applications in coordination, organometallic, and bioinorganic chemistry. *John Wiley & Sons*.

23. Albertin, G., Antoniutti, S., Bordignon, E., & Pattaro, S. (1997). Synthesis, characterisation and reactivity of hydrazine complexes of iron (II). *Journal of the Chemical Society, Dalton Transactions*, (22), 4445-4454.

24. Ommenya, F. K., Nyawade, E. A., Andala, D. M., & Kinyua, J. (2020). Synthesis, Characterization and Antibacterial Activity of Schiff Base, 4-Chloro-2-{(E)-[(4-Fluorophenyl) imino] methyl} phenol Metal (II) Complexes. *Journal of Chemistry*, *2020*(1), 1745236.

25. Kafi-Ahmadi, L., Marjani, A. P., & Pakdaman-Azari, M. (2018). Synthesis, characterization and antibacterial properties of N, N'-Bis (4-dimethylaminobenzylidene) benzene-1, 3-diamine as new Schiff Base ligand and its binuclear Zn (II), Cd (II) complexes. *South African Journal of Chemistry*, *71*, 155-159.

26. International Union of Pure and Applied Chemistry. (2014). Thermogravimetric analysis. In Compendium of Chemical Terminology (the Gold Book)

27. Montazerozohori, M., Farokhiyani, S., Masoudiasl, A., & White, J. M. (2016). Crystal structures, Hirshfeld surface analyses and thermal behavior of two new rare tetrahedral terminal zinc (II) azide and thiocyanate Schiff base complexes. *RSC advances*, *6*(28), 23866-23878.

28. Wu QianYuan, W. Q., Li Chao, L. C., Wang WenLong, W. W., He Tao, H. T., Hu HongYing, H. H., Du Ye, D. Y., & Wang Ting, W. T. (2016). Removal of fluorescence and ultraviolet absorbance of dissolved organic matter in reclaimed water by solar light.

29. Ahuja, T., Brighu, U., & Saxena, K. (2023). Recent advances in photocatalytic materials and their applications for treatment of wastewater: A review. *Journal of Water Process Engineering*, *53*, 103759.